醫工學會誌 : 第 13 卷, 第 4 號, 1992
J. of KOSOMBE : Vol. 13, No. 4

研 究 論 文
92 - 13 - 4 - 09

Numerical Studies of Flow Across End-to-Side Distal Vascular Bypass Graft Anastomoses

Y. H. Kim[1], J. H. Kim[2] and J. W. Shin[2]

=Abstract=

A numerical simulation of the steady and pulsatile flow across the end-to-side anastomosis was performed in order to understand the role of flow dynamics in the preferential development of distal anastomotic intimal hyperplasia. The finite element technique was employed to solve two-dimensional unsteady pulsatile flow in that region. The results of the steady flow revealed that low shear stresses occur at the proximally occluded host artery and at the recirculation region in the inner wall just distal to the toe region of the anastomosis. The normalized wall shear rate was increased, as was the recirculation zone size in the host artery of the by-pass graft anastomosis, with increased anastomotic junction angle. In order to minimize the size of the low wall shear region which might result in the intimal hyperplasia in the by-pass graft anastomosis, a smaller anastomotic junction angle is recommended. The pulsatile flow simulation revealed flow that regions of low and ascillating wall shear do exist near the anastomosis as in the steady simulation. The shift of stagnation point depends on the pulsation of the flow. As the flow was accelerated at systole, the stagnation point moved downstream, disappered at early diastole and reappeared during late diastole. Low shear stress was also found along both walls of the occluded proximal artery. However, the diastolic flow behavior is quite different from the steady results. The vortex near the occluded artery moved downstream and inwardly during late systole, and disappeared during diastole. Recirculations proximal to the toe and heel regions were significant during diastole. Shear stress oscillation was found along the opposite wall. The results of the present study revealed that low shear occurs at the proximally occluded host artery and the recirculation region in the inner wall just distal to the toe region of the anastomosis. The present study suggested that the regions of fluctuated wall shear stress wit flow separation is correlated with the preferential developing regions of anastomosis neointial fibrous hyperplasia.

Key Words : End-to-side anastomosis, intimal hyperplasia, wall shear stress, recirculation

INTRODUCTION

Failure in by-pass grafts replacements have been reported with losses of patent over the past 30 years. The main sources of graft failure

<접수 : 1993년 1월 15일>
School of Chemical Engineering[1] and Mechanical Engineering[2] Georgial Institute of Technology Atlanta, Ga. 30332

has been found to be intimal hyperplasia with a primary site being the distal anastomosis. Clowes et al.[1] reported that the anastomotic neointimal hyperplasia results from endothelial and smooth muscle cell proliferation. Numerous studies have suggested an important interaction between the hemodynamics and chronic development of intimal hyperplasia. The wall shear stress has been believed to be an important factor in maintaining the homeostasis of the arterial wall and regulating its reaction with blood components[2,3]. The anastomotic geometry and compliance of the graft material are major determinants of the fluid dynamics across the graft anastomosis. The presence of those complex flow pattern along the arterial wall produces a highly variable shear environment of intimal hyperplasia[4].

Many investigators[3,5-9] revealed intimal thickening or plaque developments in the region of low and oscillating shear, where have been a particular interest of intimal hyperplasia. Clinical results show that a preferred location for the development of hyperplasia is near the toe of the anastomosis and along the outer wall where the inlet stream strikes the wall[4]. The anastomosis also alters flow dynamics such that the healing response of the artery produces intimal hyperplasia. Bharadvaj et al.[10] and Kim et al.[11,12] showed that the intimal hyperplasia is greater in regions of flow separation and low shear stress. Studies by Rittgers et al.[5] and Bassiouny et al.[9] have also suggested an inverse correlation between shear rate and intimal thickness.

In vitro flow visualization studies[13,14] on models of end-to-side anastomosis such as dye injection of aluminum particles have provided useful informations on the flow dynamics in the anastomotic region. However, the limited resolution of such techniques made it difficult to obtain quantitative informations on detailed flow dynamics. Keynton et al.[8] performed In vitro experiments on the end-to-side anastomosis with various junction angle using Laser Doppler anemometry measurements. Ojha et al. [15] investigated the flow field within a rigid In vitro model of end-to-side anastomosis using a photochromic tracer technique and they also reported the correlation between the region of low wall shear or flow separation and preferential sites for the development of intimal hyperplasia. Kim[11] studied experimental and numerical studies on fluid dynamics characteristics near the compliant ena-to-end anastomosis region. He employed the axisymmetric finite element analysis to solve the two dimensional steady Navier-Stokes equation numerically and used the flush-mounted hot film anemometer to measure the wall stress near the anastomotic region. His study revealed the good correlation between the region of development of intimal hyperplasia and the low shear region. Fluid particles resides in the recirculation zone for a relatively long time, which might result in higher potential for the mass transfer across the intimal layer to created intimal hyperplasia.

The aims of the present study is to investigate the pulsatile flow dynamic behavior near the region of end-to-side anastomosis which may provide valuable relationship with regions of anastomotic intimal hyperplasia or plaque development. Effects of the anastomotic junction angle and the flow rates on the flow dynamic characteristics near the anastomotic regions were also investigated in the steady flow simulation.

METHOD

The problem domain employed in the present study is shown in Figure 1, which was similar to the in vitro experimental study by Keynton

et al.[8]. Graft of the same diameter as the host artery was anastomosed by the end-to-side anastomosis with various anastomotic junction angles of 30° , 45° and 60° for steady flow simulation, and the proximal end of the artery was occluded. A total of 1386 nodes with 1268 quadrilateral elements were used for all anastomotic geometries. A finer elemental mesh was used in the vicinity of vessel walls and near the anastomotic region. The distance from the anastomosis and velocity components in axial and radial directions were non-dimensionalized by the vessel diameter and the mean value of the inlet velocity profile respectively.

With incompressible steady laminar flow conditions, the continuity equation and momentum equation can be expressed as:

$$U_{i,i}=0 \tag{1}$$

$$\rho\left[\frac{\partial u_i}{\partial t}+u_j \cdot u_{i,j}\right]=-p_i+\mu\left[u_{i,j}+u_{j,i}\right]_j \tag{2}$$

where u_i are the velocity components, p is the pressure, μ is the dynamic viscosity and ρ is the density of the fluid. To solve the governing equations(1) and (2), the finite element method was employed. Since an Eulerian viewpoint of fluid motion is adopted in equation (1) and(2), the elements are assumed to be fixed in space. Within each element in the problem domain, the dependent variable u_i and p are interpolated by a function of compatible order, in terms of values to be determined at a set of nodal points. Within each element, the pressure and the velocity fields are approximated by

$$u_i(x)=\varphi^T U_i(t) \tag{3}$$

$$p(x)=\Psi^T P(t) \tag{4}$$

where U_i and P and the velocity and pressure vectors of nodal pointsm, and φ and Ψ are the interpolation functions. A parabolic velocity profile was employed for inlet boundary conditions and the fully developed condition was given at the downstream with no-slip condition at the wall.

Substitutions of these approximations into the governing and boundary equations yield a set of equations:

$$\text{Momentum } f_1(\varphi, \Psi, U_i, P)=R_1 \tag{5}$$

$$\text{Continuity } f_2(\varphi, U_i)=R_2 \tag{6}$$

where R_1 and R_2 are residuals(errors) resulting from the approximation of equations(3) and (4).

In order to minimize the residuals or the errors of each element, the Galerkin method of the weighted residual was used by making the residuals a to the interpolation functions of each element. These orthogonality equations are represented with inner product in the following manner:

$$(f_1, \varphi)=(R_1, \varphi) \tag{7}$$

$$(f_2, \Psi)=(R_2, \Psi) \tag{8}$$

Using the definition of Galerkin formulations (5) and (6) and the finite element approximations (3) and (4) for pressure and velocity respectively, equations (1) and (2) can be reformulated:

$$\left[\int_v \Psi \frac{\partial \varphi^T}{\partial x_i} dV\right] U_i=0$$

$$\left[\int_v \rho\varphi\varphi^T\right]\frac{dU_i}{dt}+\left[\int_v \rho\varphi u_j \frac{\partial \varphi}{\partial x_j} dV\right]U_i-\left[\int_v \frac{\partial \varphi}{\partial x_i}\Psi^T dV\right]P+\left[\int_v \mu \frac{\partial \varphi}{\partial x_j}\frac{\partial \varphi^T}{\partial x_j} dV\right]U_i$$
$$+\left[\int_v \mu \frac{\partial \varphi}{\partial x_i}\frac{\partial \varphi^T}{\partial x_i} dV\right]U_j=\int_s t_i \varphi dS$$

The above equations(9) and (10) can also be represented as matrix equations.

$$\text{Momentum: } MU+A(U)+K(U)U-CP=F \tag{11}$$

$$\text{Continuity: } C^T U=0 \tag{12}$$

A single matrix equation can be obtained by combining the above equations and their coefficients matrices can be determined by comparing equations(10) and(12).

For transient solution procedures, the forward Euler method of time integration when applied to equation (11) gives

$$U_{n+1}=U_n+dtM^{-1}[F_n-A(U_n)-K(U_n)U_n-CP_n] \tag{13}$$

Before equation (13) is used to advance the ve-

locity, the pressure at time t_n must be computed. To obtain the pressure at time t_n, the time differential version of equation(12) is used:

$$C^TU=0 \quad (14)$$

Substituting the equation (13) into equation (14), the pressure at time t_n can be evaluated:

$$(C^TM^{-1}C)P_n=C^TM^{-1}[F_n-K(U_n)U_n] \quad (15)$$

Therefore, the sequence of steps for advancing the velocity and pressure from t_n to t_{n+1} is

(a) Form the acceleration vector(ignoring the pressure gradient):

$$A_n=M^{-1}[F_n-K(U_n)U_n] \quad (16)$$

(b) Solve the linear algebraic system for compatible pressure:

$$(C^TM^{-1}C)P_n=C^TA_n \quad (17)$$

(c) Update the velocity, accunting for the pressure gradient:

$$U_{n+1}=U_n+dt(AU_n-M^{-1}CP_n) \quad (18)$$

The mean Reynolds numbers were chosen to be 100 and 205 for steady simulations, since they are found to be in coronary and femoral arteries, respectively. For the unsteady pulsatile flow study, Reynolds number of 205 was employed with the sinusodial flow wave form, as shown in Figure 2.

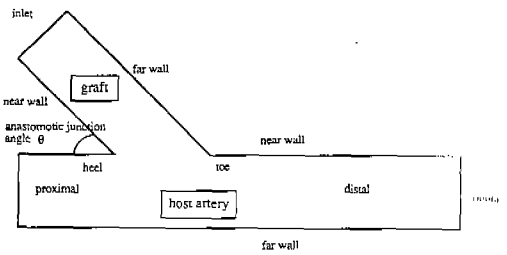

Fig. 1 Problem domain of the present study. $\theta=30°$, $45°$ and $60°$ for the steady flow and $45°$ for unsteady flow

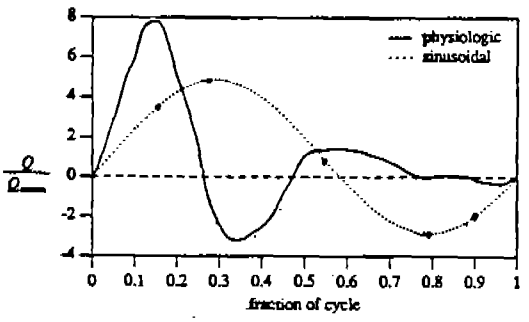

Fig. 2 Sinusoidal flow waveform in the unsteady pulsatile flow simulation. Points represent the early systole, peak systole, near zero flow, early diastole, and late diastole of the cardiac cycle.

RESULTS

Steay Flow

Velocity vectors in the vicinity of the end-to-side anastomoses are shown in Figures 3(a), (b) and (c), corresponding to various anasto-

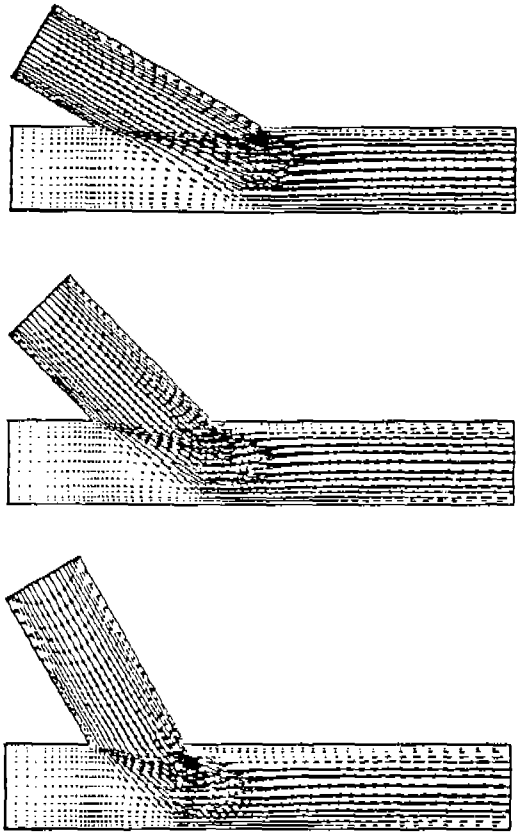

Fig. 3 Velocity vectors near the end-to-side anastomosis region.
(a) 30 deg. (b) 45 deg. (c) 60 deg.

motic junction angles of 30° , 45° and 60° . A stagnation point was found at the vessel outer wall, and at this point the flow stream splits into two parts with one stream moving in the direction of the outlet branch and the other stream moving in the direction of the occluded branch with a large clockwise vortex. Very near the proximal occluded artery, a small counter-clockwise vortex was also formed at high Reynolds number. The axial velocity profile at the distal positions of the host artery became skewed toward the outer wall for all three different geometries. Distal to the toe region of the anastomosis along the inner wall, a small flow recirculation was also found for anastomotic junction of 45° and 60° . Generally, low wall shear stress was calculated at the near wall of the vessel, and high wall shear stress occurred at the far wall. Figures 4(a) and (b) show the normalized wall shear rate at the far wall of the host artery for various anastomotic junction angles. wall shear rates were normalized by the value far downstream of the host artery. Due to the large vortex in the proximal artery, the negative wall shear was calculated along the far wall of the anastomotic junction

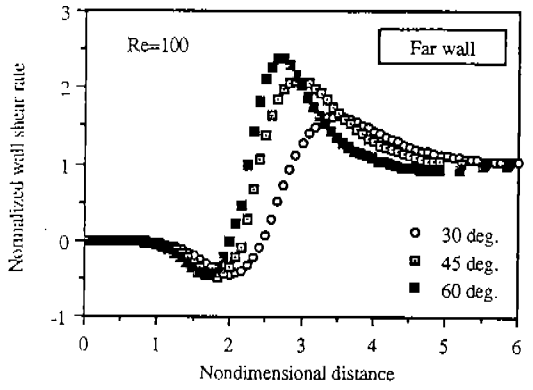

(a)

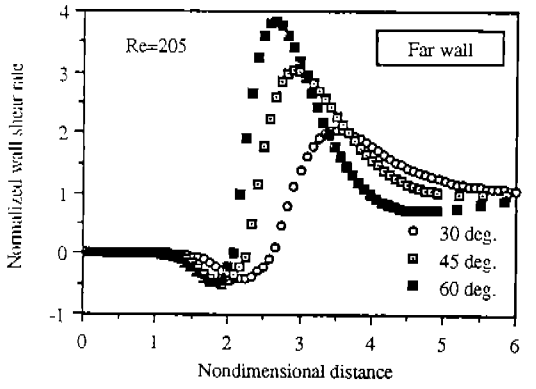

(b)

Fig. 4 Normalized wall shear rate along the outer wall of the artery.
(a) Re=100 (b) Re=205

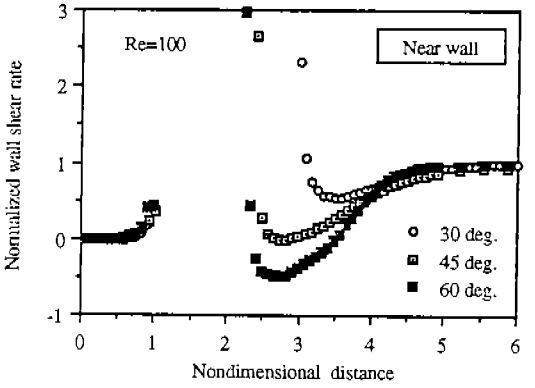

(a)

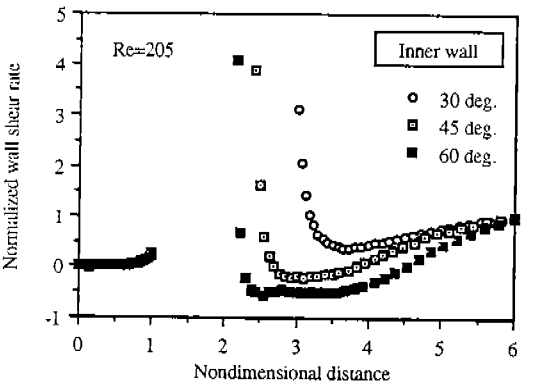

(b)

Fig. 5 Normalized wall shear rate along the inner wall of the artery.
(a) Re=100 (b) Re=205

prior to the stagnation point. Since the vortex moves proximally with increased anastomotic angles, the vortex region proximal to the anastomosis becomes smaller and thus the minimal wall shear on the far wall of the artery is located closer to the upstream at the occluded branch. However, the magnitude of those negative wall shear stress has its largest value at the anastomotic junction angle of 45° . Distal to the stagnation point, the wall stress is drastically increased as the flow hits the far wall of the artery. The maximum wall shear rate on the far wall of the host artery is evaluated at the location closer to the anastomosis with increased anastomotic junction angles.

Figures 5(a) and (b) represent the normalized wall shear rate at the inner wall of the host artery for various anastomotic junction angles. Regions of low shear stress were calculated at the inner wall of the artery except at the anastomotic junction. A flow recirculation was observed at the toe region of the graft anastomosis at 45° and 60° . With increased anastomotic junction angles, this counter-clockwise recirculation region becomes larger, the magnitude of the minimum wall shear becomes large and the minimal wall shear on the inner wall is

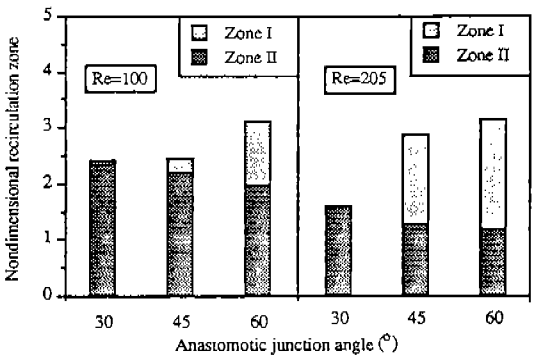

Fig. 6 Total recirculation zone near the end-to-side anastomotic region. Zone I refers the region distal to the toe of the anastomosis and Zone II refers the region near occluded artery.

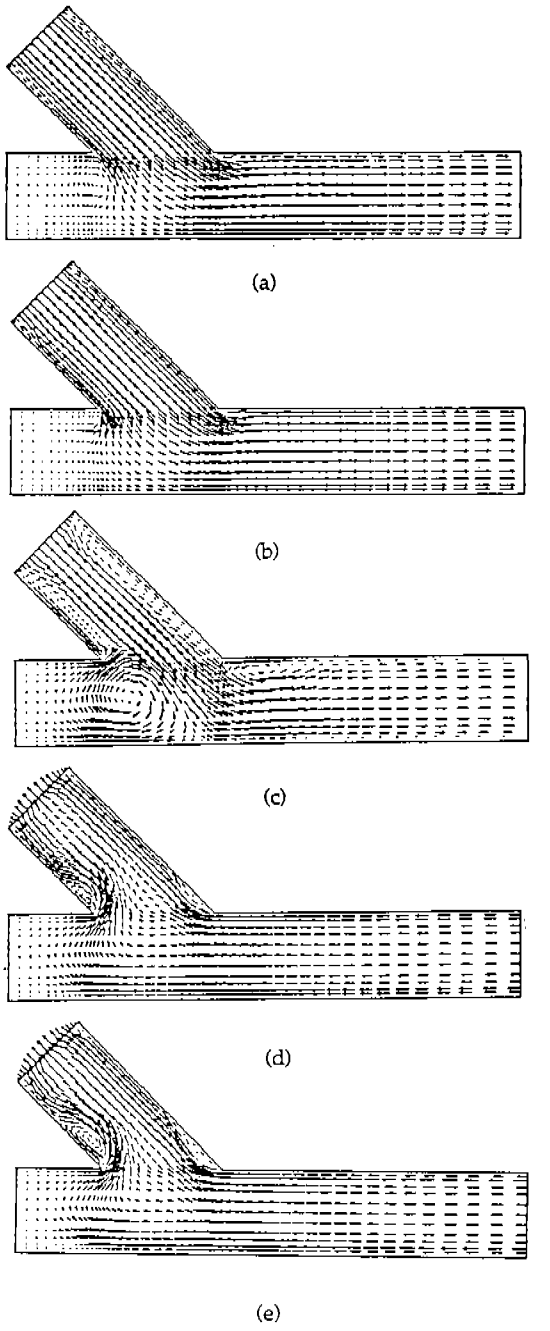

Fig. 7 Velocity vectors in the unsteady pulsatile flow.
(a) early systole (b) peak systole (c) late systole
(d) mid-diastole (e) late diastole

located closer to the anastomotic junction. It is noted that the maximal wall shear occurs at the far wall of the host artery, while the minimum wall shear occurs at the same axial location near the wall.

Figure 6 shows the total recirculation zone size with respect to the anastomitic junction angles for different flow rates. It was non-dimensionalized with respect to the width of the cannel. The size of the recirculation zone distal to the toe region of the anastomosis was increased, but the size of the vortex near the occluded artery was decreased. It is noted that the total recirculation zone size was decreased with decreased anastomotic junction angles. With increased Reynolds number, the stagnation point moved further downstream and the recirculation zone size was increased. As the anastomotic junction angle is increased, the total recirculation zone size becomes larger, thus the location of the minimal wall shear moved proximal to the occluded branch and the magnitude of the maximal wall shear was increased.

Unsteady Pulsatile Flow

The pulsatile flow simulation revealed that a low and oscillating wall shear stress exists near the anastomotic region. Figures 7(a)-(d) show velocity vector at early systole, peak systole, late systole, early diastole, and late diastole. Flow behavior during systole is relatively similar to the results for the steady state. However, the diastolic flow characteristic is quite different from the steady state results. The recirculation near the heel region is more significant at the late systole than that in the steady state simulation and it moves toward downstream. This vortex moved toward the inner wall at early diastole and disappeared during the remaining part of diastole. Instead, the recirculation just proximal to toe and heel regions are remarkable during diastole.

Similarly to the steady state results, the low shear was calculated during the entire cardiac cycle near the occluded artery, However, during late diastole, high shear stress was calculated very near the heel region. Very complicated wall shear stress patterns were found along the inner and outher walls distal to the anastomosis. During systole, low wall shear was calculated distal to the toe region and high shear was found at regions where the flow stream strikes the far wall of the host artery, which is in good agreement with the results of the steady flow. However, during diastole, relatively high wall shear was calculated at both locations.

In early systole, low shear was calculated on the inner wall of proximal artery and a tiny vortex occurred near the heel regions of the proximal artery, as seen in Figure 7(a). Due to the accelerating flow, the increased wall shear stress was calculated along the far wall across the anastomotic region. The oscillation of wall shear stress occurs as the core flow reaches the stagnation point on the far wall of the host artery during the systolic acceleration. At the maximum flow rate, the recirculation near the proximal occluded artery became stronger and maximal wall shear stress was seen at the far wall.

In the deceleration phase, the recirculation near the proximal occluded artery moved toward downstream and was increasing in strength. The wall shear stress at the far wall was decreased distal to the anastomosis and the velocity profiles were skewed toward the far wall of the host artery. A small counter-rotating vortex close to the occlusion was found at the proximal end. A small recirculation was also found at the toe region of the anastomosis. As the flow rates were decreased, the strong vortex near the proximal occluded artery moved downstream and the recirculation at the toe re-

gion became stronger. It is noted that the recirculation was found along the graft wall during diastole. At zero flow phase, only the core region of the graft maintained forward flow and the vortex at the toe region became stronger. It is noted that the strong vortex at the proximal artery moved towards the inner wall.

The stagnation point where the flow stream hits the far wall of the host artery disappeared during the diastole. During early diastole, the vortex at the proximal artery moved to the near wall of the host artery and high wall shear was found at both the heel and toe region. At late diastole, high shear was found at the toe and heel region. The vortex at the proximal artery was getting weaker and flow separation was occurred at the toe and heel region.

At any phase in the cycle, a very small wall shear was calculated near the proximal occluded artery and there is counter-clockwise vortex near the proximal end. Due to the counter-clockwise vortex near the proximal end, low positive wall shear stress was found at the near wall of the artery and negative wall shear at the far wall of the distal end. This wall shear stress becomes larger at the heel location(0.95D, D=Diameter).

Figure 8(a) shows the non-dimensional wall shear rate along the near wall of the artery. Similarly, low shear was calculated in the region close to the occlusion and the wall shear was increase as the flow moves toward the heel region. At maximum flow phase, a flow separation was found near the toe region and laminar reattachment was found at 0.5 D(Diameter) from the toe. At diastole, the wall shear along the near wall experienced negative values. It is noted that the wall shear had large fluctuations in magnitudes at the toe region. Figure 8(b) shows the non-dimensional wall shear rate along the far wall of the artery. Low shear stress was found in the region close to the occlusion during the entire cardiac cycle. A very complicated wall shear pattern was found at the far wall just across the anastomosis region where the flow stream hits the outer wall. During systole, the stagnation point on the far wall moved distal to the artery and disappeared at early diastole because fluid moved towards the graft. During this phase, the strong cloclwise rotating vortex moved upward to the anastomosis region and the flow across the toe region of the anastomosis were affected by this vorfex and thus profile was skewed towards the far wall. At the location where the flow stream hits the

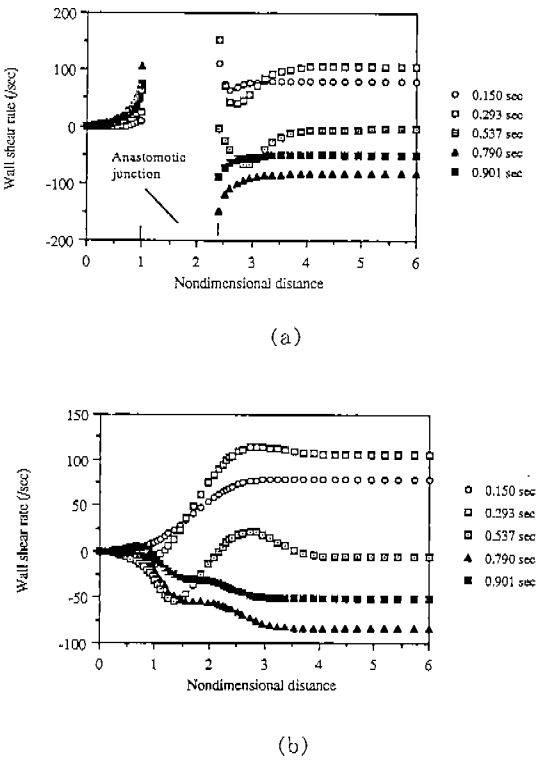

Fig. 8 Wall shear rates along the host artery. (a) Near wall (b) Far wall

far wall of the artery, the maximum(negative) wall shear rate in the pulsatile flow was approximately five times larger that in the steady flow. The movement of stagnation point on the far wall of the artery depended on the pulsation of the flow. Figure 9 shows the shift of the stagnation point according to the cardiac cycle. As flow was accelerated during systole, the stagnation point moved downstream, disappeared at early diastole and reappeared at late diastole.

Figures 10(a) and (b) show the wall shear rate along near and far wall of the graft respectively. Wall shear stress was increased during the early systole, as flow moved closer to anastomotic junction along the near wall. However, during diastole, the small positive wall shear stress was found due to the flow separation at the heel. The fluctuation of wall shear stress is significant in the vicinity of the heel of the graft. Similarly, wall shear stress along the far wall in the graft was increased as flow moves closer to the toe region. The fluctuation in the wall shear stress is also significant near toe region.

Figure 11(a) shows the wall shear rate along the near of the host artery with respect to the fractional time of the cardiac cycle. As already mentioned, wall shear was low with positive value near the occluded artery. However, at the toe region of the near wall of the artery, the wall shear present has its maximum value during the early systole, and minimal at diastolic peak. The wall shear stress downstream of the artery corresponds to the sinusoidal change of the flow characteristics. On the other hand, wall shear rate along the far wall of the host artery is shown in Figure 11(b). Small negative wall shear is noted near wall of the occluded artery. The wall shear downstream along the far wall becomes maximal with time lag equal to approximately 1/9 of a cardiac cycle. The maximal

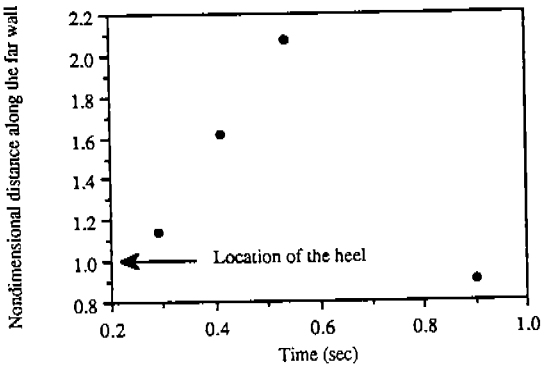

Fig. 9 Movement of the stagnation point on the far wall of the host artery

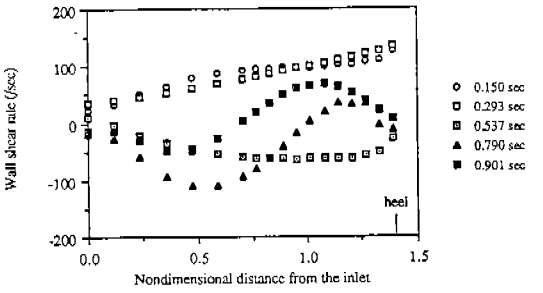

(a)

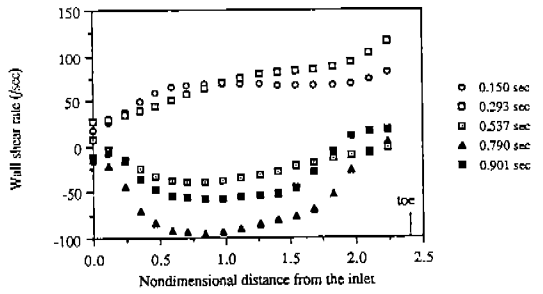

(b)

Fig. 10 Wall shear rates along the graft. (a) Near wall (b) Far wall

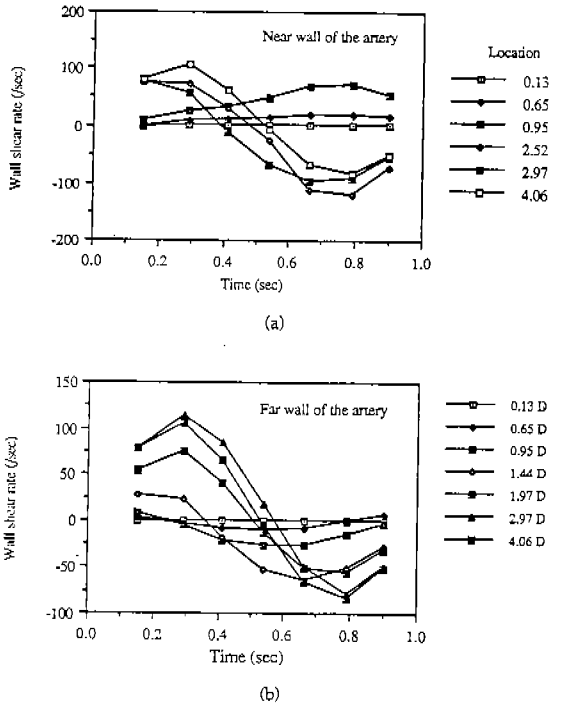

Fig. 11 Wall shear rate on the host artery as a function of time.
(a) Near wall (b) Far wall

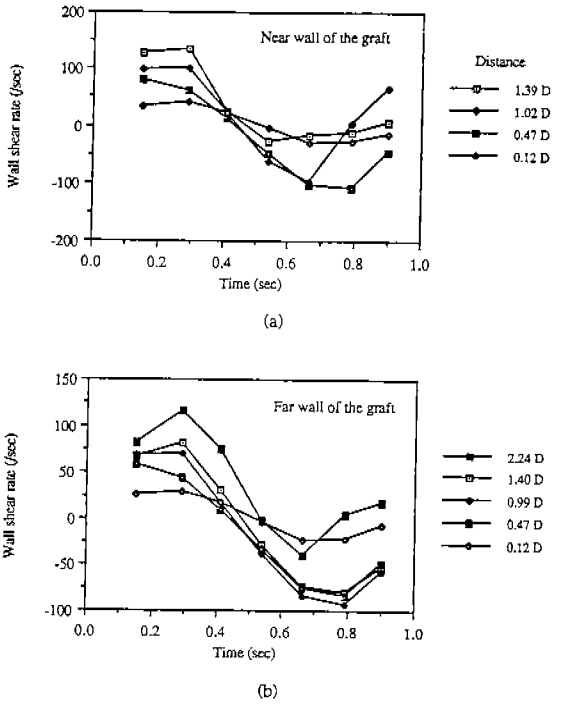

Fig. 12 Wall shear rate on the graft as a function of time.
(a) Near wall (b) Far wall

wall shear along the far wall of the host artery is found at the peak systole just proximal to the stagnation point.

Non-dimensional wall shear rates along both walls of the graft are shown in Figure 12(a) and (b). It is noted that the fluctuation of wall shear is significant near the anastomotic region close to the toe as well as the heel region. The maximal wall shear were found at the toe and the heel regions during the peak systole. Wall shear stress changes its direction corresponding to the flow, and it is generally decreased during the late systole as the time goes on.

DISCUSSION

To date, the exact etiology of the anastomotic neoinitimal hyperplasia and thrombosis are unknown. Numerous researchers have postulated that the wall shear plays an important role in this vascular diseases. Low shear stress was observed at distal locations of the toe region and upstream of the stagnation point near the occluded artery. Several investigators[4,5,8,9] have revealed that low wall shear inversely correlates with intimal thickening and suggested

that the most probable sites for the intimal hyperplasia would be these low shear regions. Some researchers have correlated intimal thickening with low mean shears in combination with high variations in shear stress[22,24]. Fry[2] also suggested that deformation, swelling, and eventual erosion of the endothelium might occur at sites where the local shear stress is relatively high. Thus, it may indicate that there are optimal range of wall shear stress variations to maintain a normal functioning of the arterial wall.

Even though this study does not incorporate clinical situations, the low shear occurs at the recirculation regions in the host artery upstream of the by-pass graft anastomosis, the stagnation points on the far wall and the recirculation region on the inner wall distal to the toe region of the anastomosis. In the canine studies, Sottiurai et al.[4] found that the greatest amount of intimal thickening in a distal graft anastomosis occurred at the near wall or toe region of the graft junction and along the wall where the inlet stream strikes the far wall. Many vascular surgeons have found that thrombotic filling occurs in the occluded branched upstream of the anastomosis, which corresponds to the region of large recirculation zones in the present numerical study. Their findings correlate well with the recirculation zone or low wall shear distal to the toe from the present study. Fluid particles reside in the recirculation zone for a relatively long time, which might result in the intimal hyperplasia. Asakura and Karino [19] also pointed out that increased particle residence time with intimal thickening. Platelets in the stagnation region of blood are prone to aggregate and release chemicals that promote aggregation and adhesion[20]. Platelet adheres and aggregates in an area where platelets might already be activated by exposed collageneous layers of vessel wall at surgery or by the artificial vascular graft material.

From the present numerical studies, a spiraling motion in the distal artery can be suggested from the fact that the high velocity exists along the outer wall and low velocity occurred along the inner wall. The secondary flow caused by the centrifugal force is expected to be strongly dependent on the angle of the anastomosis, and this geometric factor will influence the spatial and temporal variations of the fluid dynamics field. Researchers also have found that the intimal hyperplasia develops at the anastomotic junctions of vascular by-pass grafts.

Combining all the above information, the results of this study suggest that intimal hyperplasia would be expected to occur at the near wall of the anastomotic junction and at the far wall around the stagnation points. However, the stresses in the high shear regions may also induce the primary intimal hyperplasia in the low shear regions by causing endothelial cells to secrets growth factor that accumulates in the low flow regions. Recently, Giddens et al.[16] reported that the determining factor of the intimal hyperplasia may be the maxmum wall shear experienced during the cycle regardless of directions and not simply the mean shear value.

Rittgers et al[5] and Bassiouny et al.[9] implied that an anastomotic junction angle of 45° would be recommended in order to produce minimal intimal thickening with given Reynolds number. However, the present steady flow results revealed that with increased anastomotic junction angle, the absolute value of normalized wall shear on both near and far wall just distal to the anastomotic junction was increased and the recirculation zone size in the host artery upstream of the by-pass graft anastomosis was increased. However, the size of recirculation zone was increased with increased anastomotic angle

is recommended for minimizing regions of low shear.

The flow dynamics in the vicinity of the anastomosis may also depend on the compliance of the graft, suture technique and exercising condition of patients[11,12]. Binns et al.[18] also supported the importance of the graft diameter with the fact that an optimal graft diameter may contribute to the prevention of neointimal hyperplasia and pseudointimal thickening by optimizing shear stress to near normal levels. Furthermore, it is now recognized that the arterial diameter in variety of mammalian species, including humans, responds to long term changs in flow conditions such that the mean wall shear stress is maintained in a range from 10 to 20 dyne/cm^2[17,21], leading to the conclusion that arteries adapt to fluid dynamic wall shear stress in a very sensitive manner.

The present numerical study does not incorporate all of the physiological conditions of the human body, such as two-dimensional channel flow and Newtonian fluid. A simple sinusoidal flow waveform was also used for pulsatile flow simulation. In addition, the compliance mismatch between the host artery and the graft was not been considered in the simulation. In spite of all these limitations, the present study suggested that the regions of fluctuating wall shear stress with low wall shear or flow separation near an end-to-side anastomosis may be correlated with the preferential developing regions of anastomotic neointimal fibrous hyperplasia.

REFERENCES

1) Clowes, A.W., Gown, A.M. "Mechanisms of Arterial Graft Failure: I. Role of Cellular Proliferation in Early Healing of PTFE Prosthese", Am. J. Pathol. 118:43-54, 1985.

2) Fry, D.L. "Acute Vascular Endothelial Changes Associated with Increased Blood Velocity Gradients", Circulation Research, 22:175-197, 1968.

3) Caro, C.G., Fitz-Gerald, J.M., and Schroter, R.C. "Atheroma and Arterial Wall Shear: Observation, Correlation and Proposal of a Shear Dependent Mass Transfer Mechanism for Atherogenesis", Proc. R. Soc. Lond. Vol. B117, 1971, pp.109-159.

4) Sottiuri, V.S., Yao, J.S.T., and Batson, R.C. "Distal Anastomotic Intimal Hyperplasia: Histologic Character and Biogenesis", Ann. Vas. Surg., Vol. 1, 1989, pp.26-33.

5) Rittgers, S.E., Karayannacos, P.E., and Guy, J.F. "Velocity Distribution and Intimal Proliferation in Autogenous Vein Grafts in Dogs", Circ. Res., Vol. 42, 1978, pp.792-801.

6) Dobrin, P.B., Littooy, F.N., and Endean, E. D. "Mechanical Factors Predisposing to Intimal Hyperplasia and Medial Thickening in Autogeneous Vein Grafts", Surgery, Vol. 105, 1989, pp.393-400.

7) Logerfo, F.W., Soncrant, T., Teel, T., and Dewey, C.F. "Boundary Layer Separation in Models of Side-to-end Anastomosis", Archieves of Surgery, Vol. 114, 1979, pp. 1369-1373.

8) Keynton, R.S., Shu, M.C.S., and Rittgers, S. E. "The Effect of Angle and Flow Rate upon Hemodynamics in Distal Vascular Graft Anastomoses: An In Vitro Model Study", J.Biomech. Eng., 1991, pp.1421

9) Bassiouny, H.S., and Leiber, B.B. "Quantitative Inverse Correlation of Wall Shear Stress with Experimental Intimal Thickening", Surgery Forum: Cong. Am. Coll. Sourg., Oct., 1988, pp.328-329.

10) Bharadvai, B.K., and Daddaria, D.M. "Flow

Studies at Arterial Anastomoses", 35th ACEMB, Philadelphia, 1982.

11) Kim, Y.H. "Flow Dynamics in the Vicinity of End-to-end Anastomosis", Ph. D. Dissertation, University of Iowa, 1991.

12) Kim, Y.H., and Chandran, K.B., "Steady Flow Analysis in the Vicinity of an End-to-end Anastomosis", Submitted to Biorheology.

13) Crawford, H.M., Quist, W.C., Serrallach, E., Valeri, C.R., and Logerfo, F.W. "Flow Disturbance at the Distal End-to-side Anastomosis", Archieves of Surgery, Vol. 115, 1980, pp.1280-1284.

14) Watts, K.C., Marble, A.E., Sarwal, S.N., KInley, C.E., Watton, J., and Mason, M.A. "Simulation of Coronary Artery Revascuarization", J. Biomech. Vol. 19, 1986, pp. 491-499.

15) Ojha, M., Ethier, C.R., Johnston, K.W., and Cobbold. R.S.C. "Steady and Pulsatile Flow studies in an End-to-side Arterial Anastomosis Model", J. Vasc. Surg., Vol. 12, 1990, pp.747-753.

16) Giddens, D.P., Zarins, C.K., Giddens, E.M., Bassiuny, H.S., and Glagov, S. "Exercise Flow Affects Hemodynamics of End-To-Side Vascular Graft Models", Third U.S.A.-China-Japan Conference on Biomechanics, 1991, pp.66-67.

17) Zarins, C.K., Zatina, M.A., Giddens, D.P., Ku, D.N., and Glagov, S., "Shear Stress Regulation of Artery Lumne Diameter in Experimental Atherogenesis", J. Vasc. Surg., Vol. 5, 1987, pp.413-420.

18) Binns, R.L., Ku, D.N., Stewart, M.T., Ansley, J.P., and Coyle, K.A. "Optimal Graft Diameter: Effect of Wall Shear Stress on Vascular Healing", j. Vasc. Surg., Vol. 10, 1989, pp.326-337.

19) Asakura, T., and Karino, T. "Flow Patterns and Spatial Distribution of Atherrosclerotic Lesions in Human Coronary Arteries", Circ. Res., Vol. 66, 1990, pp.1045-1066.

20) Karino, T., and Goldsmith, H.L."Aggregation of Human Platelets in an Annular Vortex Distal to a Tubular Expansion", Microvasc. Res., Vol. 17, 1979, pp.217-237.

21) Giddens, D.P., Zarins, C.K., and Glagov, S. "Respons of Arteriec to Near Wall Fluid Dynamics Behavior" Appl. Mech. Rev., Vol 43, 1990, pp.S98-S102.

22) Ku, D.N., Giddens, D.P., Zarins, C.K., and Glagov, S. "Pulsatile Flow and Atherosclerosis in the Human Carotid BIfurcation: Positive Correlation Between Plaque Location and Low and Oscillating Shear Stress", Arthe-rosclerosis, Vol. 5, 1985, pp.293-302.

23) Morinaga, K., Okadome, K., Kuroki, M., Miyazaki, T., Muto, Y., and Inokuchi, K. "Effect of Wall Shear Stress on Intimal Thickening of Arterially Traksplanted Autogenous Veins in Dogs", J. Vasc. Surg., Vol. 2, 1985, pp.430-433.

24) Glagov, S., Zarins, C.K., Giddens, D.P., and Ku, D.N. "Hemodynamics and Athero-sclerosis: Insights and Perspectives Gained from Studies of Human Arteries", Archs. Path. Lab. Med., Vol. 112, pp.1018-1031.